

Valence theory

J. N. Murrell

*Professor of Chemistry
University of Sussex, England*

S. F. A. Kettle

*Lecturer in Chemistry
University of Sheffield, England*

J. M. Tedder

*Professor of Chemistry
Queen's College, University of St. Andrews, Scotland*

1965

JOHN WILEY & SONS LTD
London New York Sydney

Copyright © 1965 by John Wiley & Sons Ltd.

All rights reserved

Library of Congress catalog card number 65-25154



B 40 129

Set in 10 on 12 point Monotype Times by Santype Ltd. of Salisbury
and printed in Great Britain by Western Printing Services Ltd., Bristol.

Preface

This book has been written for honours chemistry undergraduates and for graduate students not specializing in theoretical chemistry. It is meant to bridge the gap between the semiquantitative picture given in Coulson's *Valence* and the formal mathematical account given in Eyring, Walter and Kimball's *Quantum Chemistry*—two books which we greatly admire.

It has been assumed that the student has acquired elsewhere an elementary knowledge of differential calculus and vector algebra. There are some points in the chapter on symmetry which need a slight knowledge of matrix algebra.

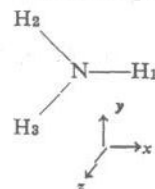
The book has been based on lectures given for the past four years at the University of Sheffield. Our experience has been that the student only obtains a full grasp of the subject when he has successfully tackled some problems, and we consider that the problems in this book are an essential part of the text; some of the problems provide proofs of statements made in the text. A student benefits most if he is given the minimum of help necessary to enable him to solve the problem. To take a step in this direction we have provided hints to the problems at the end of the book. The student should first try the problems without the hints, but with their help most students should be able to obtain the solutions.

The first five chapters are intended for first year students, since we feel that an early grasp of such concepts as the orbital and the electron-pair bond are necessary for any course in experimental chemistry. The more formal mathematical aspects of the book start in chapter 6 when it has been assumed that the student has received some mathematical training during his first year. These later chapters also assume a knowledge of other branches of chemistry.

Inevitably we have had to omit some topics on the fringe of valence theory. Spectroscopy and the theory of the solid state are the two major omissions but we feel that both these require books of their own for an adequate presentation. For the same reason we have made only scanty reference to the theory of intermolecular forces.

We have only given references to work which we think the student might wish to examine in more detail, and to acknowledge numerical data that we have quoted. There are plenty of advanced texts which provide a full list of references to the subject.

- 12.2 The following are the N—H bonding molecular orbitals for NH_3 .† What are the equivalent orbitals?



$$\begin{aligned}\psi_1 &= 0.76 \text{ } 2s + 0.16 \text{ } 2p_z - 0.27 \text{ } H_0 \\ \psi_2 &= 0.62 \text{ } 2p_x + 0.49 \text{ } H_x \\ \psi_3 &= 0.62 \text{ } 2p_y + 0.49 \text{ } H_y\end{aligned}$$

where $H_0 = \sqrt{\frac{1}{3}}(h_1 + h_2 + h_3)$
 $H_x = \sqrt{\frac{1}{6}}(2h_1 - h_2 - h_3)$
 $H_y = \sqrt{\frac{1}{6}}(h_2 - h_3)$

- 12.3 What is the expression for the energy of H_2O in the perfect-pairing VB scheme?

- 12.4 Write down a Heitler-London wave function for linear BeH_2 and deduce the valence state of the Be.

Chapter 13

Ligand-field theory

13.1 Simple crystal-field theory

The interesting chemistry of transition metal ions is largely that of their complexes. In the majority of these complexes a transition metal cation is surrounded by six molecules or anions (collectively called *ligands*) arranged at the corners of a more or less regular octahedron. This six-fold coordination occurs in many structures where at first sight it appears unlikely. For example, crystals of $\text{CuSO}_4 \cdot 5\text{H}_2\text{O}$ and FeCl_3 both contain octahedrally-coordinated cations as shown in figure 13.1. In the first

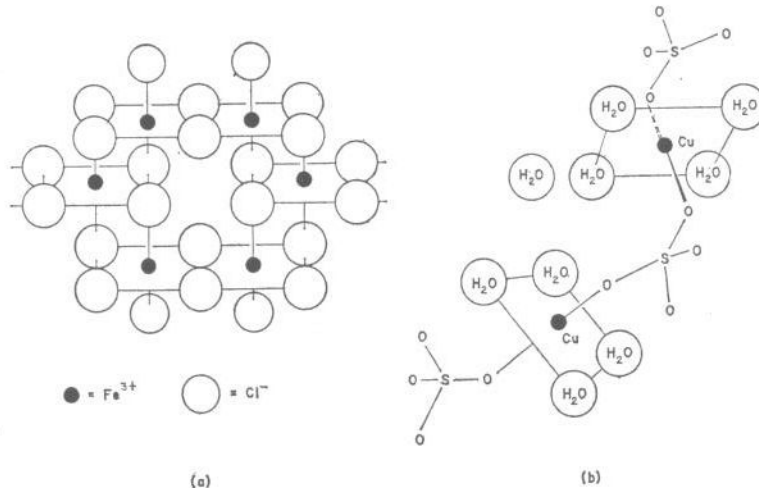


FIGURE 13.1. Octahedral coordination in FeCl_3 and $\text{CuSO}_4 \cdot 5\text{H}_2\text{O}$

transition series (Ti to Cu) ions with from four to seven *d* electrons form two sets of complexes, one with more unpaired electrons present than the other. This is clearly shown by the electronic spectra of these complexes. For example, divalent iron ($3d^6$) forms both green $[\text{Fe}(\text{H}_2\text{O})_6]^{2+}$ and

† KAPLAN, *J. Chem. Phys.*, **26**, 1704 (1957).

yellow $[\text{Fe}(\text{CN})_6]^{4-}$ complexes. The former has four unpaired electrons for each iron atom and is paramagnetic; the latter has no unpaired electrons and is diamagnetic.

Three theories have been advanced to explain these differences; in all of them the occupation of the d orbitals of the cation is of paramount importance. The first theory to gain general acceptance was the VB approach due to Pauling. He suggested that octahedrally-coordinated transition metal ions are either d^2sp^3 (i.e. $3d^2 4s 4p^3$) or sp^3d^2 (i.e. $4s 4p^3 4d^2$) hybridized and these hybrid orbitals are used to form bonds with the ligands. In the first case, three of the $3d$ orbitals are not used to form hybrids. In the second case, all five $3d$ orbitals are unused. This means that in the first case there is a maximum of three unpaired d electrons, and in the second five, which accounts for two forms of complexes. This theory has largely fallen into disuse although its nomenclature is sometimes encountered—viz. ‘inner’ (using $3d$ orbitals for the hybrids) and ‘outer’ orbital complexes (using $4d$ orbitals). Its most serious drawback is that it makes no mention of antibonding orbitals and in consequence cannot explain electronic spectra and it cannot account for the existence of fairly stable ‘inner orbital’ complexes with more than six d electrons. Despite its considerable contribution to the understanding of the chemistry of metal complexes, we shall not discuss it further here†.

A more satisfactory approach is provided by either crystal- or ligand-field theory. The former is an entirely electrostatic theory first introduced by van Vleck, the latter a mixture of electrostatic and MO theories. Crystal- and ligand-field calculations have much in common, so we shall discuss the former in some detail before explicitly introducing molecular orbitals.

Crystal-field theory regards the electrostatic attraction between the ionic or highly polar ligand (e.g. Cl^- , H_2O) and the positively charged cation as responsible for the stability of a complex. The forces involved are similar to those which hold an ionic crystal together—hence the name of the theory. The essential step made by the theory is the recognition that, although in an isolated cation the degeneracy of all five d orbitals is maintained, in an octahedral crystal field the degeneracy is removed.

It is usual to choose the cartesian axes of an octahedral complex to be the four-fold axes of the octahedron. It follows that p orbitals are still degenerate in the complex, for all have exactly equivalent positions with respect to the ligands. This is not true for the d orbitals. Two, $d_{x^2-y^2}$ and d_{z^2} , point along the axes whilst the other three, d_{xy} , d_{yz} and d_{zx} , are directed

† The interested reader is referred to the account given in PAULING, *Nature of the Chemical Bond*, 2nd. ed., Cornell, 1962.

between the axes. These sets will have different energies†. If the field of the ligands is approximately that of point negative charges, then clearly an electron in d_{xy} , d_{yz} or d_{zx} will have a lower energy than one in d_{z^2} or $d_{x^2-y^2}$. This is illustrated in figure 13.2. The part of the potential which affects both sets equally is not important and its effect is omitted from the figure.

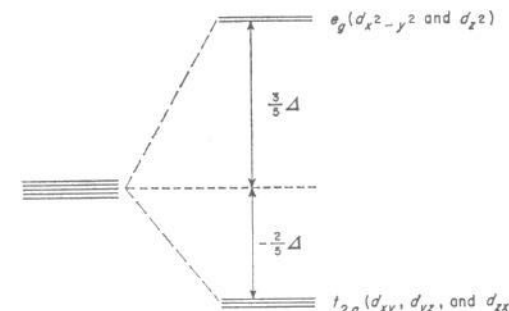


FIGURE 13.2. The splitting of d orbitals in an octahedral crystal field

In figure 13.2 the two sets of d orbitals are labelled by the I.R.’s of the octahedral group \mathbf{O}_h under which they transform. (It is common to use lower case group theory symbols to label orbitals and upper case for states.) Alternative labelling which may be encountered replaces e_g by either d_y or γ_3 ; t_{2g} by d_e or γ_5 .

The separation between the t_{2g} and e_g orbitals is denoted by Δ (or $10 Dq$)‡. Δ varies from complex to complex, but for any ion it is possible to

† On page 24 we pointed out that d_{z^2} and $d_{x^2-y^2}$ were in fact equivalent although they looked different.

‡ If the potential is expanded in terms of spherical harmonics (3.6) then the first terms which can remove the degeneracy of the d orbitals are those having $l = 4$. Expressing these in cartesian coordinates we get $V_{\text{oct}} = D(x^4 + y^4 + z^4 - \frac{3}{5} r^4)$ where D is $\frac{35e^2Z}{4a^5}$, assuming that the ligands act as point charges Ze at a distance a from the cation. The separation between the two sets of d orbitals is then $\frac{5e^2Z\bar{r}^4}{3a^5}$ where \bar{r} is the mean distance of a d electron from the cation

nucleus. It is usual to write $\frac{5e^2Z\bar{r}^4}{3a^5}$ as $10Dq$, where $q = \frac{Z\bar{r}^4}{105}$. $10Dq$ is, then, an entirely theoretical quantity. We prefer to use Δ , and regard it entirely as an empirical quantity.

list ligands in order of the magnitude of Δ which they produce. It is found that this list is almost identical no matter which ion is considered. Since Δ is usually determined spectroscopically, the list is called the *spectrochemical series*. An abbreviated series is



Δ is about $12,000 \text{ cm}^{-1}$ for divalent and $20,000 \text{ cm}^{-1}$ for trivalent ions of the first transition series. Ions of the second and third series have rather larger values.

A consideration of figure 13.2 provides a simple explanation of the magnetic anomalies mentioned at the beginning of this chapter without involving the rather ad hoc change in bond type of valence-bond theory. The electron configuration of the di- and tri-positive cations of the elements titanium to copper are shown in table 13.1. We have to feed from one to nine electrons into the e_g and t_{2g} orbitals. There is a competition

TABLE 13.1 The number of $3d$ electrons in the di- and tri-positive ions of the elements titanium to copper. None of these ions have any $4s$ or $4p$ electrons

	Ti	V	Cr	Mn	Fe	Co	Ni	Cu
M^{2+}	2	3	4	5	6	7	8	9
M^{3+}	1	2	3	4	5	6	7	8

between the energy to be gained by having electrons in different orbitals (thus maximizing exchange energy and minimizing coulomb repulsion) and the energy to be gained by having all electrons in the lowest set of orbitals. Two limiting cases can be distinguished: Δ can be small (the 'high-spin' or 'weak-field' case) or Δ can be large (the 'low-spin' or 'strong-field' case). In the weak-field case, electrons are added successively as shown in figure 13.3, the energy gap Δ being small enough to allow Hund's rule to be obeyed. The spin multiplicity is therefore the same as that for the ground state of the free gaseous ion, reaching a maximum at the d^5 configuration.

When Δ is large the crystal-field energy dominates and the electron configurations shown in figure 13.4 are obtained.

In crystal-field theory it is therefore the balance between electron-interaction energies and the crystal-field energy which determines the magnetic properties of a complex. Another factor will become apparent when we consider ligand-field theory—the extent of σ and π bonding. The nomenclature of the two classes of complexes should by now be evident.

	—	—	—	—	↑	↑	↑	↑	↑
	—	—	—	↑	↑	↑	↑	↑	↑↓
	—	—	↑	↑	↑	↑	↑	↑	↑↓
	—	↑	↑	↑	↑	↑	↑	↑↓	↑↓
	↑	↑	↑	↑	↑	↑	↑	↑↓	↑↓
Number of unpaired electrons	1	2	3	4	5	4	3	2	1
Spin multiplicity	2	3	4	5	6	5	4	3	2

FIGURE 13.3. The electron distribution in weak-field (high-spin) complexes (but see page 217)

	—	—	—	—	—	—	—	↑	↑
	—	—	—	—	—	—	—	↑	↑
	—	—	↑	↑	↑	↑	↑	↑↓	↑↓
	—	↑	↑	↑	↑	↑	↑	↑↓	↑↓
	↑	↑	↑	↑	↑	↑	↑	↑↓	↑↓
Number of unpaired electrons	1	2	3	2	1	0	1	2	1
Spin multiplicity	2	3	4	3	2	1	2	3	2

FIGURE 13.4. The electron distribution in strong-field (low-spin) complexes

'High spin' and 'low spin' are phenomenological terms, 'weak field' and 'strong field' describe the magnitude of the crystal field.

Crystal-field theory also provides a simple explanation for the regularities found in the heats of formation of series of complexes when the central cation is varied. Since an electron in a t_{2g} orbital is stabilized by $\frac{2}{3}\Delta$ with respect to the energy zero (which is taken to be the average crystal-field energy of all the d orbitals), and an electron in an e_g orbital is destabilized by $\frac{1}{3}\Delta$; we can calculate the total stabilization for any electron configuration. The results of such a calculation are given in table 13.2 for weak-field complexes. An analogous table can be compiled for strong-field complexes.

As an example we consider the heats of hydration of divalent ions of the first transition series. The experimental results lie on two curves, intersecting

TABLE 13.2. Crystal-field stabilization energies for weak-field octahedral complexes

Number of <i>d</i> electrons	Electron configuration	Crystal-field stabilization energy
0	$t_{2g}^0 e_g^0$	0
1	$t_{2g}^1 e_g^0$	$-\frac{1}{2}\Delta$
2	$t_{2g}^2 e_g^0$	$-\frac{2}{3}\Delta$
3	$t_{2g}^3 e_g^0$	$-\frac{3}{4}\Delta$
4	$t_{2g}^4 e_g^1$	$-\frac{3}{4}\Delta$
5	$t_{2g}^5 e_g^2$	0
6	$t_{2g}^6 e_g^2$	$-\frac{1}{2}\Delta$
7	$t_{2g}^7 e_g^2$	$-\frac{2}{3}\Delta$
8	$t_{2g}^8 e_g^2$	$-\frac{3}{4}\Delta$
9	$t_{2g}^9 e_g^3$	$-\frac{3}{4}\Delta$
10	$t_{2g}^{10} e_g^4$	0

in a minimum at Mn^{2+} . If the calculated crystal-field stabilization energy appropriate to each ion is subtracted (Δ being obtained from the electronic spectrum of the hydrate), an almost straight line results. This is shown in figure 13.5†.

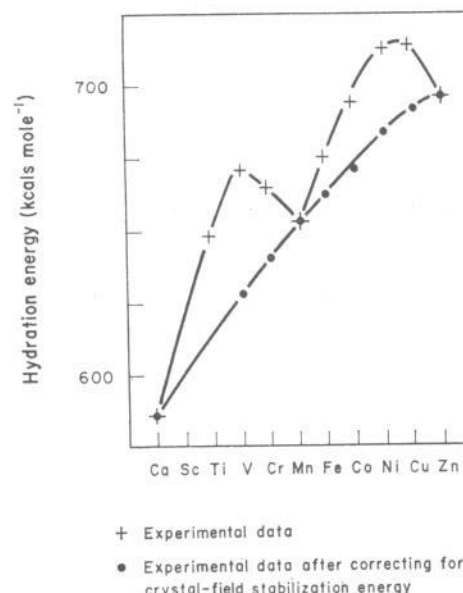


FIGURE 13.5. Experimental and corrected heats of hydration of divalent ions of the first transition series

† For a fuller discussion and for more examples, the reader is referred to GEORGE and MCCLURE, *Prog. Inorg. Chem.*, **1**, 381 (1959).

13.2 The detailed crystal-field theory of weak-field complexes

We now consider in more detail the effect of the crystal field on *d* orbitals. Crystal-field theory neglects any overlap between ligand and cation orbitals and considers only the effect of an electrostatic perturbation on the latter.

In calculating the energy levels of an isolated atom or ion in the Russell-Saunders scheme (page 110) one first considers the coulomb attraction between each electron and the nucleus, then the electron-electron repulsions, then spin-orbit coupling, this being the order of decreasing importance (figure 9.2). Crystal-field theory follows exactly the same pattern, but at an appropriate point in the development the crystal-field perturbation is inserted. For first row transition metal ions, this insertion takes place either before the electron-interaction stage (strong-field complexes) or before spin-orbit coupling (weak-field complexes). Even the weakest crystal field found in practice is strong compared with spin-orbit coupling, although this is not necessarily true for the other transition series and is certainly not true for the rare earths. The terms given by a d^n configuration in the Russell-Saunders scheme may be found by the methods described in chapter 9. The ground states are determined by Hund's rules and are listed in table 13.3.

TABLE 13.3. Ground state terms of the $d^1 \rightarrow d^9$ configurations

Configuration	d^1	d^2	d^3	d^4	d^5	d^6	d^7	d^8	d^9
Free-ion ground state	2D	3F	4F	5D	6S	5D	4F	3F	2D

We shall now consider the effect of a weak field on these ground states. Since an electrostatic field does not interact directly with electron spin we need only consider how the crystal field removes the orbital degeneracy. Apart from the d^5 configuration, only *D* and *F* terms appear in table 13.3 and we can cover these by discussing the d^1 and d^2 cases; the rest, apart from d^5 , will then have been dealt with.

A *D* state has five-fold orbital degeneracy, and an *F* state seven-fold. However, one can see from group theory that an orbital degeneracy of no more than three can persist in an octahedron (the O_h character table, given in table 13.4, shows no degeneracy greater than three) so that both *D* and *F* terms must split into at least two and three components respectively in an octahedral complex. Using group theory we shall first see how the *D* state splits up.

TABLE 13.4. The character table of the groups O_h

O_h	I	$6C_4$	$3C_2$	$6C_2'$	$8C_3$	i	$6S_4$	$3\sigma_h$	$6\sigma_d$	$8S_6$
A_{1g}	1	1	1	1	1	1	1	1	1	1
A_{1u}	1	1	1	1	1	-1	-1	-1	-1	-1
A_{2g}	1	-1	1	-1	1	1	-1	1	-1	1
A_{2u}	1	-1	1	-1	1	-1	1	-1	1	-1
E_g	2	0	2	0	-1	2	0	2	0	-1
E_u	2	0	2	0	-1	-2	0	-2	0	1
T_{1g}	3	1	-1	-1	0	3	1	-1	-1	0
T_{1u}	3	1	-1	-1	0	-3	-1	1	1	0
T_{2g}	3	-1	-1	1	0	3	-1	-1	1	0
T_{2u}	3	-1	-1	1	0	-3	1	1	-1	0

Clearly, the five components of a D state have the same symmetry properties as the five d orbitals since the symbols d and D both indicate an angular variation described by the spherical harmonics with $l = 2$. Any symmetry operation of the group transforms one of the components of the state into a mixture of the five. It follows that these five components form a basis for a representation of the group, and we want to know the component $I.R.$'s of this representation (page 91).

The character of the representation is the sum of the diagonal elements of the matrix which represents the operation of the group on the D states. This is given simply by the sum of the parts of each component which are unchanged by the operation. Let us take two easy ones to start with: the identity operation leaves all five components unchanged hence $\chi(I) = 5$; the inversion operator also leaves the sign of each component unchanged (d orbitals have g symmetry) hence $\chi(i) = 5$. The results of the other operations are more difficult to see, but we can get the answers by considering the general effect of a rotation by an angle φ on the states.

Suppose we want to find the effect of a rotation about a particular axis in space. There are many ways of choosing wave functions for the components of the D state (d orbitals) because all five components are degenerate. Clearly, we want to choose those wave functions which make this particular problem as simple as possible. This is done by arbitrarily taking the axis we are concerned with as the z axis and also taking the wave functions in complex form (3.9). The rotation we are considering only changes the reference point for the polar variable φ , and the five components depend on φ in the following manner (see 3.9)

$$e^{2i\varphi}, e^{i\varphi}, 1, e^{-i\varphi}, e^{-2i\varphi}.$$

If we rotate by an angle α these functions become

$$e^{2i(\varphi+\alpha)}, e^{i(\varphi+\alpha)}, 1, e^{-i(\varphi+\alpha)}, e^{-2i(\varphi+\alpha)},$$

hence we can say, for example,

$$R_x e^{2i\varphi} = e^{2i\alpha} \cdot e^{2i\varphi}, \quad (13.1)$$

or uniting the effect on all five components in matrix form

$$R_x \begin{pmatrix} e^{2i\varphi} \\ e^{i\varphi} \\ 1 \\ e^{-i\varphi} \\ e^{-2i\varphi} \end{pmatrix} = \begin{pmatrix} e^{2i\alpha} & 0 & 0 & 0 & 0 \\ 0 & e^{i\alpha} & 0 & 0 & 0 \\ 0 & 0 & 1 & 0 & 0 \\ 0 & 0 & 0 & e^{-i\alpha} & 0 \\ 0 & 0 & 0 & 0 & e^{-2i\alpha} \end{pmatrix} \begin{pmatrix} e^{2i\varphi} \\ e^{i\varphi} \\ 1 \\ e^{-i\varphi} \\ e^{-2i\varphi} \end{pmatrix}. \quad (13.2)$$

The character of the matrix which represents this operation on the components of the D states is therefore

$$e^{2i\alpha} + e^{i\alpha} + 1 + e^{-i\alpha} + e^{-2i\alpha} = \frac{\sin \frac{5\alpha}{2}}{\sin \frac{\alpha}{2}}. \quad (13.3)†$$

We can generalize this result to find the character for any state with a quantum number L whose $2L+1$ components have a φ dependence $e^{iL\varphi}, e^{i(L-1)\varphi} + \dots e^{-iL\varphi}$. The required character is

$$e^{iL\alpha} + e^{i(L-1)\alpha} + \dots e^{-iL\alpha} = \frac{\sin(2L+1) \frac{\alpha}{2}}{\sin \frac{\alpha}{2}}. \quad (13.4)$$

We return now to the O_h group. To find the character appropriate to the operation C_4 on the D states we take the C_4 axis as the z axis and then from the formula (13.3) with $\alpha = 90^\circ$ we find $\chi(C_4) = \sin 225^\circ / \sin 45^\circ = -1$. Likewise C_2 and C_2' (both $\alpha = 180^\circ$) have characters 1, and lastly the C_3 operation ($\alpha = 120^\circ$) (again considering the components defined with the C_3 axis as z axis) has a character $\chi(C_3) = \sin 300^\circ / \sin 60^\circ = -1$.

These characters are sufficient to establish that the component $I.R.$'s are of the form $E + T_2$, but they do not determine whether the suffixes should be g or u . Because the D states which concern us are derived from d^n

† This is proved by summing the left-hand side as a geometrical progression.

configurations, and because d orbitals are centrosymmetric, it follows that the component $I.R.$'s are $E_g + T_{2g}$. The D state derived from the p^2 configuration also gives rise to E_g and T_{2g} components in an octahedral ligand field, but those derived from the pd configuration give E_u and T_{2u} components.

Following the same method (problem 13.2) the F states split up under an octahedral field to give components $T_{1g} + T_{2g} + A_{2g}$. We now have to determine the relative energies of the components of the D and F terms. We start by considering the d^1 case. We already know how the orbitals split up, and this is summarized in table 13.5.

If the electron occupies the t_{2g} orbitals a $^2T_{2g}$ state results, if it occupies the e_g orbitals we get a 2E_g state. We shall write these wave functions in complex form as follows $(l, m_l) = (2,2), (2,1), (2,0), (2,-1), (2,-2)$; and the real forms of the wave functions are then given as in table 13.5.

TABLE 13.5. Wave functions and energies from the d^1 configuration in an octahedral field

Real orbital	Wave function (see table 3.1)	Crystal-field energy
d_{z^2}	$\sqrt{\frac{1}{2}}\{(2,2) + (2,-2)\} \quad (2,0)$	$\frac{3}{5}\Delta$
d_{xy}	$-i\sqrt{\frac{1}{2}}\{(2,2) - (2,-2)\}$	
d_{yz}	$-i\sqrt{\frac{1}{2}}\{(2,1) - (2,-1)\}$	
d_{zx}	$\sqrt{\frac{1}{2}}\{(2,1) + (2,-1)\}$	$-\frac{3}{5}\Delta$

The perturbation to the energies of these orbitals due to the crystal field is given by the following expressions (put $\mathcal{H}' = V_{\text{oct}}$ in 6.50)

$$\int d_{x^2-y^2}^* V_{\text{oct}} d_{x^2-y^2} dv \\ = \frac{1}{2} \int [(2,2) + (2,-2)]^* V_{\text{oct}} [(2,2) + (2,-2)] dv = \frac{3}{5}\Delta. \quad (13.5)$$

Similarly

$$\left. \begin{aligned} \int (2,0)^* V_{\text{oct}}(2,0) dv &= \frac{3}{5}\Delta \\ \frac{1}{2} \int [(2,2) - (2,-2)]^* V_{\text{oct}} [(2,2) - (2,-2)] dv &= -\frac{2}{5}\Delta \\ \frac{1}{2} \int [(2,1) - (2,-1)]^* V_{\text{oct}} [(2,1) - (2,-1)] dv &= -\frac{2}{5}\Delta \\ \frac{1}{2} \int [(2,1) + (2,-1)]^* V_{\text{oct}} [(2,1) + (2,-1)] dv &= -\frac{2}{5}\Delta \end{aligned} \right\} \quad (13.6)$$

where, for example,

$$d_{xy}^* = \frac{i}{\sqrt{2}} [(2,2)^* - (2,-2)^*]^\dagger.$$

These integrals can be expanded (except the second, which does not need expanding). The first, for example, gives

$$\frac{1}{2} \left[\int (2,2)^* V_{\text{oct}}(2,2) dv + \int (2,2)^* V_{\text{oct}}(2,-2) dv \right. \\ \left. + \int (2,-2)^* V_{\text{oct}}(2,-2) dv + \int (2,-2)^* V_{\text{oct}}(2,2) dv \right] = \frac{3}{5}\Delta.$$

But if we either use the result that $(2,-2)^* = (2,2)$ (from 3.9) or note that $\int d_{x^2-y^2}^* V_{\text{oct}} d_{xy} dv = 0$ then

$$\int (2,2)^* V_{\text{oct}}(2,2) dv + \int (2,-2)^* V_{\text{oct}}(2,2) dv = \frac{3}{5}\Delta.$$

We are now in a position to calculate the effect of the octahedral field on the complex d orbitals. By combining expressions (13.5 and 6), we obtain,

$$\left. \begin{aligned} \int (2,2)^* V_{\text{oct}}(2,2) dv &= \frac{1}{10}\Delta \\ \int (2,1)^* V_{\text{oct}}(2,1) dv &= -\frac{2}{5}\Delta \\ \int (2,0)^* V_{\text{oct}}(2,0) dv &= \frac{3}{5}\Delta \\ \int (2,-1)^* V_{\text{oct}}(2,-1) dv &= -\frac{2}{5}\Delta \\ \int (2,-2)^* V_{\text{oct}}(2,-2) dv &= \frac{1}{10}\Delta \end{aligned} \right\} \quad (13.7)$$

† Since we are now working with complex functions we must always remember to take the complex conjugate in the first function of any integral of the type $\int \psi^* B \psi dv$.

$$\int (2,-2)^* V_{\text{oct}}(2,2) dv = \frac{1}{2} \Delta. \quad (13.8)$$

Note particularly the last integral; it is the only cross-term which is non-zero. The complete set of interaction integrals is most conveniently represented as a table or matrix (13.9)[†]

$$\begin{array}{ccccc} (2,2) & (2,1) & (2,0) & (2,-1) & (2,-2) \\ \begin{pmatrix} (2,2)^* & \frac{1}{10}\Delta & 0 & 0 & \frac{1}{2}\Delta \\ (2,1)^* & 0 & -\frac{2}{5}\Delta & 0 & 0 \\ (2,0)^* & 0 & 0 & \frac{3}{5}\Delta & 0 \\ (2,-1)^* & 0 & 0 & 0 & -\frac{2}{5}\Delta \\ (2,-2)^* & \frac{1}{2}\Delta & 0 & 0 & \frac{1}{10}\Delta \end{pmatrix} \end{array} \quad (13.9)$$

We have now expressed our crystal-field splittings in terms of complex orbitals rather than real. This is of no help in discussing the simple d^1 case (because of the cross-term between (2,2) and (2,-2)), but it will enable us to work out the energies in the d^2 case.

The eigenfunctions of the 3F term arising from the d^2 configuration are readily obtained by the shift operator method described in chapter 9. The crystal-field calculation based on these is quite simple but is rather lengthy, so we shall give it in outline only. The two-electron F eigenfunctions may be labelled (3,3), (3,2), (3,1), (3,0), (3,-1), (3,-2) and (3,-3), in conformity with the nomenclature used for d^1 .

The crystal-field perturbation does not act on spin so we can examine just one of the spin components (say $M_s = 1$). We shall give one example to show how the interaction integrals for these two-electron functions are evaluated. The function (3,3) can only arise from a combination of one electron in the d orbital (2,2) and one in (2,1). We can write this wave function in determinantal form.

$$(3,3) = |(2,2)(2,1)| = \sqrt{\frac{1}{2}}[(2,2)_1(2,1)_2 - (2,2)_2(2,1)_1], \quad (13.10)$$

where both electrons have α spin, and we label them by the subscripts 1 and 2. Then,

$$\begin{aligned} & \int (3,3)^* V_{\text{oct}}(3,3) dv \\ &= \frac{1}{2} \iint [(2,2)_1(2,1)_2 - (2,2)_2(2,1)_1]^* V_{\text{oct}} [(2,2)_1(2,1)_2, \\ & \quad - (2,2)_2(2,1)_1] dv_1 dv_2 \end{aligned} \quad (13.11)$$

[†] Because the name is readily comprehensible, we call integrals of the form (13.7) 'interaction integrals'. In the literature and in other texts the name 'matrix element' is used, an integral such as (13.8) being referred to as an 'off-diagonal matrix element'. The reason for this is obvious from an inspection of (13.9).

but since V_{oct} acts on each electron independently $V_{\text{oct}} = V_{\text{oct}}(1) + V_{\text{oct}}(2)$ and (13.11) is equal to

$$\int (2,1)_2^* V_{\text{oct}}(2)(2,1)_2 dv_2 + \int (2,2)_1^* V_{\text{oct}}(1)(2,2)_1 dv_1. \quad (13.12)$$

The values of these two integrals can be obtained from (13.7), so we have

$$\int (3,3)^* V_{\text{oct}}(3,3) dv = -\frac{2}{5}\Delta + \frac{1}{10}\Delta = -\frac{3}{10}\Delta. \quad (13.13)$$

Proceeding in this way, all of the perturbation energies can be evaluated. The results are collected together in the perturbation matrix (13.14).

$$\begin{array}{ccccccc} (3,3) & (3,2) & (3,1) & (3,0) & (3,-1) & (3,-2) & (3,-3) \\ \begin{pmatrix} (3,3)^* & -\frac{3}{10}\Delta & 0 & 0 & \sqrt{\frac{3}{20}}\Delta & 0 & 0 \\ (3,2)^* & 0 & \frac{7}{10}\Delta & 0 & 0 & \frac{1}{2}\Delta & 0 \\ (3,1)^* & 0 & 0 & -\frac{1}{10}\Delta & 0 & 0 & \sqrt{\frac{3}{20}}\Delta \\ (3,0)^* & 0 & 0 & 0 & -\frac{3}{5}\Delta & 0 & 0 \\ (3,-1)^* & \sqrt{\frac{3}{20}}\Delta & 0 & 0 & 0 & -\frac{1}{10}\Delta & 0 \\ (3,-2)^* & 0 & \frac{1}{2}\Delta & 0 & 0 & 0 & \frac{7}{10}\Delta \\ (3,-3)^* & 0 & 0 & \sqrt{\frac{3}{20}}\Delta & 0 & 0 & -\frac{3}{10}\Delta \end{pmatrix} \end{array} \quad (13.14)$$

As in the d^1 case, functions differing by four in M_L are mixed, and the crystal-field interaction between (3,3) and (3,-1) is the same as that between (3,-3) and (3,1).

To obtain the final eigenfunctions and eigenvalues, we have to solve the secular equations (6.67)

$$\sum c_i (\mathcal{H}_{ik} - ES_{ik}) = 0, \text{ where } \mathcal{H} = V_{\text{oct}}.$$

If the matrix is rearranged as in (13.15) it is clear that only 2×2 secular determinants need to be solved.

$$\begin{array}{ccccccc} (3,3) & (3,-1) & (3,-3) & (3,1) & (3,2) & (3,-2) & (3,0) \\ \begin{pmatrix} (3,3)^* & -\frac{1}{10}\Delta & \sqrt{\frac{3}{20}}\Delta & & & & \\ (3,-1)^* & \sqrt{\frac{3}{20}}\Delta & -\frac{1}{10}\Delta & & & & \\ (3,-3)^* & & & -\frac{1}{10}\Delta & \sqrt{\frac{3}{20}}\Delta & & \\ (3,1)^* & & & \sqrt{\frac{3}{20}}\Delta & -\frac{1}{10}\Delta & & \\ (3,2)^* & & & & & \frac{7}{10}\Delta & \frac{1}{2}\Delta \\ (3,-2)^* & & & & & \frac{1}{2}\Delta & \frac{7}{10}\Delta \\ (3,0)^* & & & & & & -\frac{3}{5}\Delta \end{pmatrix} \end{array} \quad (13.15)$$

Carrying out this operation in the usual way we obtain the eigenfunctions and eigenvalues given in table 13.6.

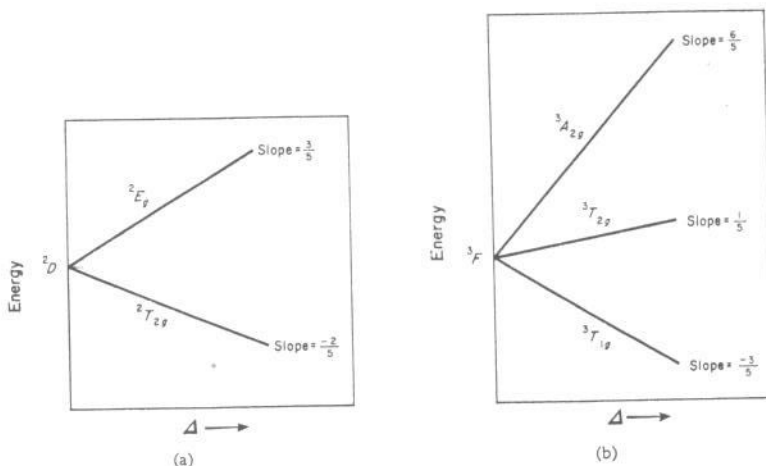
TABLE 13.6. The components of ${}^3F(d^2)$ under O_h^a

Eigenfunction	Energy	Symmetry (see table 13.4)
$\sqrt{\frac{1}{2}}(3,-1) + \sqrt{\frac{1}{2}}(3,3)$	$-\frac{3}{5}\Delta$	${}^3T_{1g}$
$\sqrt{\frac{1}{2}}(3,1) + \sqrt{\frac{1}{2}}(3,-3)$ (3,0)		
$\sqrt{\frac{1}{2}}(3,-1) - \sqrt{\frac{1}{2}}(3,3)$	$\frac{1}{5}\Delta$	${}^3T_{2g}$
$\sqrt{\frac{1}{2}}(3,1) - \sqrt{\frac{1}{2}}(3,-3)$		
$\sqrt{\frac{1}{2}}[(3,2) + (3,-2)]$	$\frac{6}{5}\Delta$	${}^3A_{2g}$
$\sqrt{\frac{1}{2}}[(3,2) - (3,-2)]$		

^a We have evaluated wave functions for the case of both electrons having α spin. These are one component of each triplet state. The spin multiplicity is written as a prefix to the symmetry label.

It is convenient to show the data in tables 13.5 and 13.6 graphically. This is done in figure 13.6.

Figure 13.6 can readily be modified to include other configurations with D or F ground states. Consider the 4F ground state of the d^3 configuration

FIGURE 13.6. The splitting of D and F terms in an octahedral crystal field

as an example. The d^3 configuration differs from spherical symmetry (d^5) by two 'holes'. The splitting of the resulting ${}^4F(d^3)$ term will be exactly the same as for the ${}^3F(d^2)$ term except that V_{oct} , which repels electrons, will attract holes. Figure 13.6(b) has therefore to be inverted for ${}^4F(d^3)$. Analogous arguments show that figure 13.6(b) is correct for ${}^4F(d^7)$ but should be

inverted for ${}^3F(d^8)$. Similarly, figure 13.6(a) is correct for ${}^5D(d^6)$ but has to be inverted for ${}^5D(d^4)$ and ${}^2D(d^9)$.

It remains to discuss the ground state of the d^5 configuration, which is 6S . Since this is orbitally non-degenerate, it cannot be split by a crystal field.

There is an interesting consequence of our discussion of the weak-field ${}^3F(d^2)$ case. The ground state is stabilized by $-\frac{3}{5}\Delta$ with respect to the arbitrary zero. What occupation of t_{2g} and e_g orbitals is required to give this stabilization? From figure 13.2 we see that the occupation numbers must be $\frac{9}{5}$ in the t_{2g} and $\frac{1}{5}$ in the e_g orbitals ($\frac{1}{5} \times \frac{3}{5}\Delta - \frac{9}{5} \times \frac{2}{5}\Delta$). In the weak-field d^2 case electron repulsion pushes a small amount of electron density into the unstable e_g orbital. It follows that in our earlier discussion of the magnetic properties of complex ions we were not quite correct in allocating two electrons to t_{2g} orbitals in the weak-field d^2 case. However, the small correction we deduce here is barely detectable in an experiment.

Non-integral occupation of t_{2g} and e_g orbitals is also found for weak-field ${}^7(^4F)$ octahedral and ${}^3(^4F)$ and ${}^8(^3F)$ tetrahedral complexes.

13.3 Strong-field complexes

We now turn to a consideration of strong-field complexes. In order to do this we need to consider all of the terms which arise from a configuration, not just the ground term, because when Δ is large the ground state of the complex does not necessarily arise from the ground state of the free ion, and second-order perturbation energies become important.

Excited orbitally-degenerate terms of a configuration are split by a crystal field in just the same way as the ground term. Table 13.7 lists the terms arising from d^n configurations. Table 13.8 lists the components of all terms, up to thirteen-fold orbitally degenerate, in the presence of an octahedral crystal field.

TABLE 13.7. Terms arising from d^n configurations. ${}^2F(2)$ means that there are two 2F terms

Configuration	Terms
$d^1 d^9$	2D
$d^2 d^8$	${}^3F, {}^3P, {}^1G, {}^1D, {}^1S$
$d^3 d^7$	${}^4F, {}^4P, {}^2H, {}^2G, {}^2F, {}^2D(2), {}^2P$
$d^4 d^6$	${}^5D, {}^3H, {}^3G, {}^3F(2), {}^3D, {}^3P(2), {}^1I, {}^1G(2), {}^1F, {}^1D(2), {}^1S(2)$
d^5	${}^6S, {}^4G, {}^4F, {}^4D, {}^4P, {}^2I, {}^2H, {}^2G(2), {}^2F(2), {}^2D(3), {}^2P, {}^2S$

TABLE 13.8. Splitting of terms in an octahedral field

Term	Orbital degeneracy $=2L + 1$	Components under O_h
S	1	A_{1g}
P	3	T_{1g}
D	5	$E_g + T_{2g}$
F	7	$A_{2g} + T_{1g} + T_{2g}$
G	9	$A_{1g} + E_g + T_{1g} + T_{2g}$
H	11	$E_g + 2T_{1g} + T_{2g}$
I	13	$A_{1g} + A_{2g} + E_g + T_{1g} + 2T_{2g}$

The eigenfunctions and energies of the components of each of these terms could be found by the method described earlier for the components of $^3F(d^2)$, but the results would only have significance if Δ were small. The reason for this is best illustrated by two examples. The terms arising from a d^5 configuration are sixteen in number, of which eleven are doublets (2I , 2H , $^2G(2)$, $^2F(2)$, $^2D(3)$, 2P and 2S); in the presence of an octahedral crystal field these split to give four $^2A_{1g}$, three $^2A_{2g}$, seven 2E_g , eight $^2T_{1g}$ and ten $^2T_{2g}$ levels. In weak fields the ground state is $^6A_{1g}$, but one of the $^2T_{2g}$ levels becomes the ground state in strong fields. In order to determine how its energy depends on Δ , we apparently have to solve a 10×10 secular determinant and select the lowest root. Fortunately, as we shall see, the problem is greatly simplified when Δ is much greater than the electron repulsion energies—which is the strong-field limit. In the more common ‘intermediate’ field region, it is simplest to interpolate between the weak- and strong-field results. The d^5 case is, of course, a particularly difficult one. Much simpler are the d^2 and d^8 configurations, for here there is only one excited level to interact with the ground state. For d^2 and d^8 an upper component of the free-ion ground term (3F) interacts with one component of an excited term (3P), both of these having T_{1g} symmetry. This has important spectral consequences because the two components are close together. We shall consider the d^2 configuration in some detail.

We label the two $^3T_{1g}$ levels according to their parentage. In our earlier discussion of the weak-field case, we ignored the existence of the excited $^3T_{1g}(^3P)$ state. Since the 3P level is not split by the crystal field (see table 13.8), the energy of this zeroth-order term is independent of Δ . Because $^3T_{1g}(^3F)$ and $^3T_{1g}(^3P)$ are of the same symmetry, there will be a cross-term

$$\int ^3T_{1g} * (^3P) V_{\text{oct}} ^3T_{1g}(^3F) dv \quad (13.16)$$

which, following the procedure described on pages 214–5, can be shown to have the value $\frac{2}{3}\Delta$.

We now want to know the difference in energy between the two terms in the free ion. In terms of the Slater–Condon parameters (9.52) this is $15F_2 - 75F_4$, which we shall simply carry through the equations as a parameter X . Taking the energy of the 3F term of the free ion as zero, the interaction integrals are given by the following matrix

$$\begin{matrix} & ^3T_{1g}(^3F) & ^3T_{1g}(^3P) \\ ^3T_{1g}(^3F) & \left(\begin{array}{cc} -\frac{3}{5}\Delta & \frac{2}{5}\Delta \\ \frac{2}{5}\Delta & X \end{array} \right) \end{matrix}. \quad (13.17)$$

The solutions of the secular determinant

$$\begin{vmatrix} -\frac{3}{5}\Delta - E & \frac{2}{5}\Delta \\ \frac{2}{5}\Delta & X - E \end{vmatrix} = 0 \quad (13.18)$$

$$\text{are } E = \frac{1}{2}[X - \frac{3}{5}\Delta \pm (X^2 + \frac{6}{5}X\Delta + \Delta^2)^{\frac{1}{2}}]. \quad (13.19)$$

In the weak-field limit $X \gg \Delta$ we have, after a binomial expansion of the square root up to terms of order Δ , $E = X$ or $-\frac{3}{5}\Delta$. This is also the result obtained by ignoring the interaction between the 3F and 3P term. In the strong-field limit $\Delta \gg X$ we have, after expansion to terms of order X ,

$$E = \frac{4X}{5} + \frac{\Delta}{5}, \quad \frac{X}{5} - \frac{4\Delta}{5}. \quad (13.20)$$

Figure 13.7 is the same as figure 13.6(b), modified to include the effect of the 3P term. Both $^3T_{1g}$ levels are curved, the limiting slope of the lower level being $-\frac{4}{5}$, and that of the upper $\frac{1}{5}$. The $^3A_{2g}$ state crosses the upper $^3T_{1g}$ if Δ is large enough. For V^{3+} , where $X = 13,200 \text{ cm}^{-1}$ this occurs when $\Delta = 11,000 \text{ cm}^{-1}$. This phenomenon will be of importance when we discuss the electronic spectrum of $[V(H_2O)_6]^{3+}$.

Strong-field complexes differ in spin multiplicity from weak-field complexes because a component from an excited term of the free ion is rapidly stabilized as Δ increases, until it eventually becomes the ground state. For example, in the d^5 case a $^2T_{2g}(^2D)$ component replaces $^6A_{1g}$ as the ground state. The latter has zero slope (being the only component of the orbitally non-degenerate 6S term), whilst the former ultimately has a slope of -2 . In the strong-field limit we no longer base our wave functions on the terms of the free ion, but on configurations built up from the crystal-field-split d orbitals (table 13.5). In this limit the $^2T_{2g}(^2D)$ level corresponds to a t_{2g}^5 configuration, that is, we have a ‘hole’ in one of the t_{2g} orbitals.

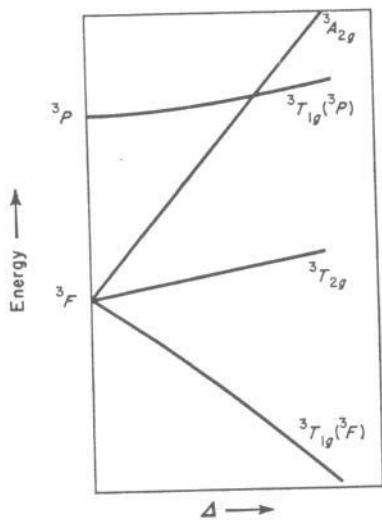


FIGURE 13.7. The effect of second-order interaction on the ground state of a d^2 octahedral complex

The variation of the energy of this level with Δ is obtained by allowing $-\frac{2}{5}\Delta$ for each electron in the t_{2g} orbitals, i.e. $5 \times (-\frac{2}{5}\Delta) = -2\Delta$.

A similar analysis holds for all other strong-field states, ground or excited. For example, d^7 gives rise to the ground configuration $t_{2g}^6 e_g^1$, and this has an energy which varies with Δ as $6(-\frac{2}{5}\Delta) + \frac{3}{5}\Delta = -\frac{9}{5}\Delta$. Likewise, the slope of the ground state for d^2 is $-\frac{4}{5}\Delta$, which is the limit we found earlier (13.20).

As an example of a wave function in the strong-field limit we again take t_{2g}^2 . The ground state is ${}^3T_{1g}$. If we consider the spin component with $M_s = 1$, then there are only three ways of allocating electrons to these three orbitals with this spin restriction, so that these must represent the three space components of the T_{1g} state. We can write them

$$|\phi_1\phi_2|, |\phi_2\phi_3|, |\phi_3\phi_1|,$$

where ϕ_1 , ϕ_2 and ϕ_3 are any three independent functions for the t_{2g} orbitals, e.g. d_{xy} , d_{yz} and d_{zx} or $(2,1)$, $(2,-1)$ and $\sqrt{\frac{1}{2}}\{(2,2) - (2,-2)\}$.

Following the method given in this and the last section crystal-field energy diagrams can be constructed for all of the d orbital configurations. Two typical cases are shown in figures 13.8 and 13.9†.

† Other cases may be found in GRIFFITH, *The Theory of Transition Metal Ions*, C.U.P., 1961.

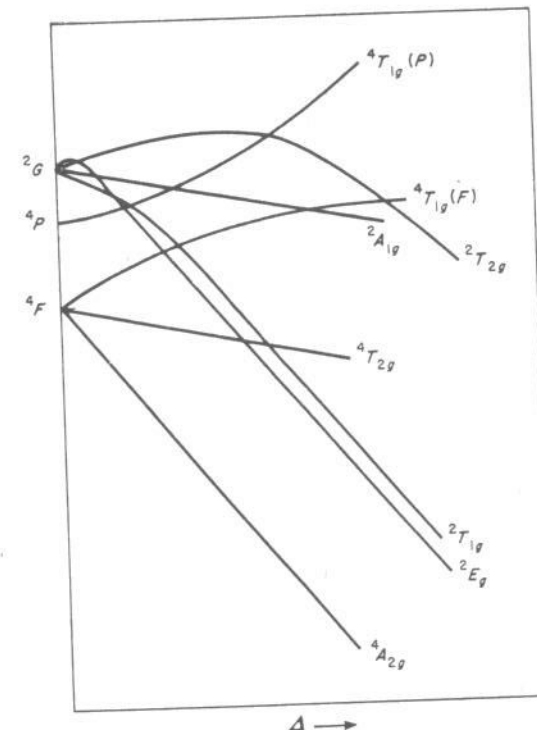


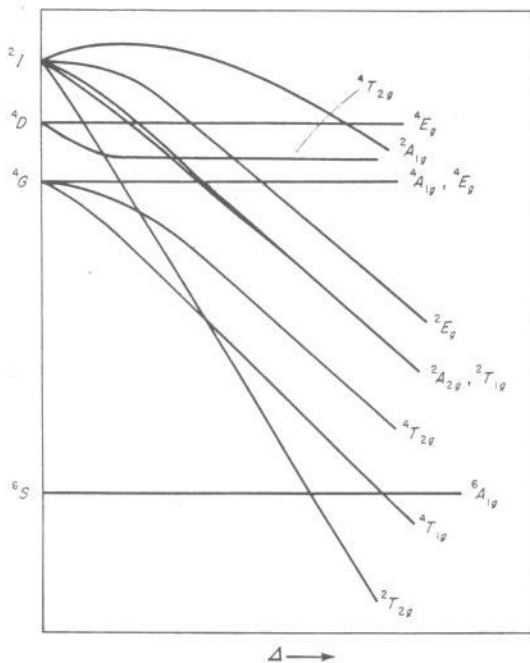
FIGURE 13.8. Crystal-field energy diagram for a d^3 configuration

13.4 Spin-orbit coupling

Although spin-orbit coupling is invariably weaker than the crystal-field interaction in the ions of the first transition series, it frequently has to be taken into account for a detailed understanding of the electronic spectra and magnetic properties of complexes.

We have already outlined the calculation of spin-orbit coupling energies in chapter 9 where we introduced the operator $\mathbf{L}\cdot\mathbf{S}$ (9.16, 9.19), and showed how this gave rise to the Landé interval rule. After the introduction of a crystal-field perturbation J and L are no longer good quantum numbers so that expression (9.20) can no longer be used. In order to calculate the spin-orbit coupling interactions, we must look in more detail at the form of the integrals involving the operator $\mathbf{L}\cdot\mathbf{S}$. These are most easily evaluated using the following expansion

$$\begin{aligned} \mathbf{L}\cdot\mathbf{S} &= \mathbf{L}_z\mathbf{S}_z + \mathbf{L}_x\mathbf{S}_x + \mathbf{L}_y\mathbf{S}_y \\ &= \mathbf{L}_z\mathbf{S}_z + \frac{1}{2}\{(\mathbf{L}_x + i\mathbf{L}_y)(\mathbf{S}_x - i\mathbf{S}_y) + (\mathbf{L}_x - i\mathbf{L}_y)(\mathbf{S}_x + i\mathbf{S}_y)\} \\ &= \mathbf{L}_z\mathbf{S}_z + \frac{1}{2}\{\mathbf{L}_+\mathbf{S}_- + \mathbf{L}_-\mathbf{S}_+\}, \end{aligned} \quad (13.21)$$

FIGURE 13.9. Crystal-field energy diagram for a d^5 configuration

where the shift operators \mathbf{L}_+ etc. are defined by (9.21).

We shall evaluate two integrals as examples[†].

$$\begin{aligned}
 (a) \int (2,1,\alpha)^* \mathbf{L}_+ \mathbf{S}(2,1,\alpha) d\tau &= \int (2,1,\alpha)^* \{ \mathbf{L}_z \mathbf{S}_z + \frac{1}{2} (\mathbf{L}_+ \mathbf{S}_- + \mathbf{L}_- \mathbf{S}_+) \} (2,1,\alpha) d\tau \\
 &= \int (2,1,\alpha)^* \mathbf{L}_z \mathbf{S}_z (2,1,\alpha) d\tau \\
 &= \int (2,1)^* \mathbf{L}_z (2,1) dv \int \alpha^* \mathbf{S}_z \alpha ds \\
 &= \left(1 \cdot \frac{h}{2\pi} \right) \left(\frac{1}{2} \cdot \frac{h}{2\pi} \right) = \frac{h^2}{8\pi^2}.
 \end{aligned}$$

[†] We have included the spin wave functions in the integrals in an obvious manner.

$$\begin{aligned}
 (b) \int (2,1,\alpha)^* \mathbf{L}_- \mathbf{S}(2,2,\beta) d\tau &= \int (2,1,\alpha)^* \{ \mathbf{L}_z \mathbf{S}_z + \frac{1}{2} (\mathbf{L}_+ \mathbf{S}_- + \mathbf{L}_- \mathbf{S}_+) \} (2,2,\beta) d\tau \\
 &= \int (2,1,\alpha)^* (\frac{1}{2} \mathbf{L}_- \mathbf{S}_+) (2,2,\beta) d\tau \\
 &= \frac{1}{2} \int (2,1)^* \mathbf{L}_- (2,2) dv \int \alpha^* \mathbf{S}_+ \beta ds \\
 &= \frac{1}{2} \frac{h}{2\pi} [(2+2)(2-2+1)]^{\frac{1}{2}} \cdot \frac{h}{2\pi} [(\frac{1}{2}-\frac{1}{2}+1)(\frac{1}{2}+\frac{1}{2})]^{\frac{1}{2}} = \frac{h^2}{4\pi^2}.
 \end{aligned}$$

The eigenvalues of the operator $\mathbf{L.S}$ for single d electron wave functions are given in matrix form below in units of $(h/2\pi)^2$. It should be noted that cross-terms (off-diagonal terms) only occur between functions with the same value of $M_J = M_L + M_S$. Many-electron spin-orbit coupling integrals can always be expressed as a sum of one-electron terms, using a technique similar to that which we adopted to evaluate two-electron integrals involving V_{oct} .

$$(2,2,\alpha)(2,2,\beta)(2,1,\alpha)(2,1,\beta)(2,0,\alpha)(2,0,\beta)(2,-1,\alpha)(2,-1,\beta)(2,-2,\alpha)(2,-2,\beta)$$

$$\begin{pmatrix}
 (2,2,\alpha)^* & 1 & . & . & . & . & . & . & . & . & . \\
 (2,2,\beta)^* & . & -1 & 1 & . & . & . & . & . & . & . \\
 (2,1,\alpha)^* & . & 1 & \frac{1}{2} & . & . & . & . & . & . & . \\
 (2,1,\beta)^* & . & . & . & -\frac{1}{2} & \sqrt{\frac{1}{2}} & . & . & . & . & . \\
 (2,0,\alpha)^* & . & . & . & \sqrt{\frac{3}{2}} & 0 & . & . & . & . & . \\
 (2,0,\beta)^* & . & . & . & . & 0 & \sqrt{\frac{3}{2}} & . & . & . & . \\
 (2,-1,\alpha)^* & . & . & . & . & . & \sqrt{\frac{3}{2}} & -\frac{1}{2} & . & . & . \\
 (2,-1,\beta)^* & . & . & . & . & . & . & . & \frac{1}{2} & 1 & . \\
 (2,-2,\alpha)^* & . & . & . & . & . & . & . & 1 & -1 & . \\
 (2,-2,\beta)^* & . & . & . & . & . & . & . & . & . & 1
 \end{pmatrix} \quad (13.22)$$

Using these results, the number of spin-orbit components for the ground and lowest excited levels of weak-field octahedral complexes are found to be as shown in the following table.

	$^1A_{1g}$	$^6A_{1g}$	$^3A_{2g}$	$^4A_{2g}$	2E_g	5E_g	$^4T_{1g}$	$^5T_{1g}$	$^2T_{2g}$	$^3T_{2g}$	$^5T_{2g}$
Number of spin-orbit components	1	1	1	1	1	1	3	3	2	3	3

For example, the weak-field complexes of $\text{Ni}^{2+}(d^8)$ have a $^3A_{2g}$ ground state and $^3T_{2g}$ and $^3T_{1g}$ excited states. These are split by spin-orbit coupling

into 1, 3 and 3 sub-levels respectively. If the splittings are large enough they may be observable spectroscopically, resulting in a splitting of one of the bands in the electronic absorption spectrum. A splitting has been observed in the ${}^3A_{2g} \rightarrow {}^3T_{1g}(F)$ transition of the $[Ni(H_2O)_6]^{2+}$ ion and has been attributed to spin-orbit coupling.

13.5 Molecular-orbital theory

Crystal-field theory suffers from the obvious limitation that it neglects the overlap between the ligand and transition metal orbitals, and if the ligand is a non-polar species (e.g. $CH_2=CH_2$) then this is likely to be more important than the electrostatic perturbation. In fact, even if one takes a realistic crystal-field potential for the polar ligands and ignores overlap effects it is difficult to obtain quantitatively correct answers from crystal-field theory. We turn now to MO theory which introduces a delocalization of electrons between the transition metal and ligand. When this is combined with crystal-field theory one obtains what is known as ligand-field theory.

We could just plunge in and form molecular orbitals by taking linear combinations of ligand and metal orbitals. This would only require the solution of, say, a 30×30 secular determinant. The problem is really much simplified by using group theory. We first take combinations of the metal orbitals which form a basis for an I.R. of the group; do the same for the ligand orbitals, and then combine ligand and metal orbitals which belong to the same I.R.

We have already seen how the d orbitals transform under the operations of the octahedral group. The same procedure can be used for other orbitals of this group, and other common symmetry groups of metal complexes. The data likely to be needed are collected in table 13.9.

TABLE 13.9. Transformation properties of atomic orbitals

	O_h	T_d	D_{3d}	D_{4h}	D_{2h}
s	a_{1g}	a_1	a_{1g}	a_{1g}	a_g
p_x	t_{1u}	t_2	a_{2u}	a_{2u}	b_{1u}
p_y			e_u	e_u	b_{3u}
d_{z^2}	e_g	e	e_g	a_{1g}	a_g
$d_{x^2-y^2}$				b_{1g}	a_g
d_{xy}	t_{2g}	t_2	a_{1g}	b_{2g}	b_{1g}
d_{yz}					b_{3g}
d_{zx}					b_{2g}

We now turn our attention to the ligand orbitals of σ symmetry (s orbitals and p orbitals pointing towards the cation). The first step is to determine the I.R.'s having these orbitals as basis. Using the method described earlier (asking how many orbitals are unchanged on each operation), we obtain the following characters of the representation.

I	$6C_4$	$3C_2$	$6C_2'$	$8C_3$	i	$6S_4$	$3\sigma_h$	$6\sigma_d$	$8S_6$
6	2	2	0	0	0	0	4	2	0

This reducible representation has components $A_{1g} + E_g + T_{1u}$.

We now use the method given in chapter 8 for obtaining the linear combinations of ligand orbitals (which we shall call ligand group orbitals) which transform according to these I.R.'s. We fix our attention on one ligand orbital and ask how it transforms under the forty-eight separate operations of the group. If we label the ligands A \rightarrow F as shown in figure 13.10 and look at A, we obtain the first line in table 13.10. To obtain, for example, the t_{1u} ligand group orbitals, we multiply the orbitals under an operation by the t_{1u} character for that operation and then add the results together. These steps are shown in table 13.10.

TABLE 13.10. The determination of t_{1u} ligand group orbitals

	I	$6C_4$	$3C_2$	$6C_2'$	$8C_3$
A becomes	A	$2A + B + C + E + F$	$A + 2D$	$2D + B + C + E + F$	$2B + 2C + 2E + 2F$
T_{1u}	3	1	-1	-1	0
Multiply	3A	$2A + B + C + E + F$	$-A - 2D$	$-2D - B - C - E - F$	—
	i	$6S_4$	$3\sigma_h$	$6\sigma_d$	$8S_6$
A becomes	D	$2D + B + C + E + F$	$2A + D$	$2A + B + C + E + F$	$2B + 2C + 2E + 2F$
T_{1u}	-3	-1	1	1	0
Multiply	-3D	$-2D - B - C - E - F$	$2A + D$	$2A + B + C + E + F$	—
Add		$8A - 8D$			
Normalize		$\psi'(t_{1u}) = \sqrt{\frac{1}{2}}(A - D)$			

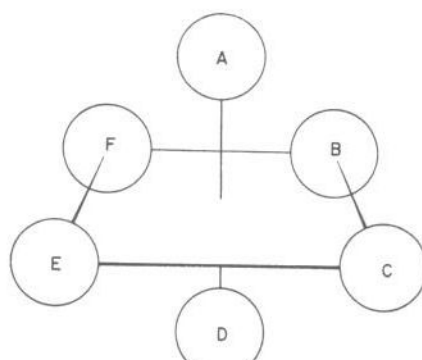


FIGURE 13.10. Labelling scheme for the ligand orbitals of an octahedral complex

The other t_{1u} ligand group orbitals are obtained by considering the transformation of B or E and C or E (D gives $\psi'(t_{1u})$ again) and are obviously

$$\psi''(t_{1u}) = \sqrt{\frac{1}{2}}(B - E)$$

$$\psi'''(t_{1u}) = \sqrt{\frac{1}{2}}(C - F).$$

These orbitals are shown in figure 13.11, along with the atomic p orbitals. It is obvious that the two sets have identical symmetry, which is just what the common t_{1u} label tells us.

The a_{1g} and e_g ligand group orbitals are obtained in a similar way. For the latter set we can generate three orbitals, which, like d_{x^2} , d_{y^2} and d_{z^2} , are not linearly independent. But suitable linear combinations of two of these can be taken to form two which are independent (page 101). The a_{1g} and e_g ligand group orbitals are

$$\psi(a_{1g}) = \sqrt{\frac{1}{6}}(A + B + C + D + E + F)$$

$$\psi'(e_g) = \frac{1}{2}(B - C + E - F)$$

$$\psi''(e_g) = \sqrt{\frac{1}{2}}(2A - B - C + 2D - E - F).$$

These are shown in figure 13.12 along with their atomic-orbital counterparts.

We can now construct a molecular-orbital energy level diagram as in figure 13.13 for a complex of the first row transition series. This is highly qualitative. We have assumed that the main interaction is between the highest occupied orbitals of the ligand and the partly filled d and empty s and p orbitals of the cation. Further, we have assumed that the ligand orbitals all have a lower energy than the d orbitals of the cation. This is

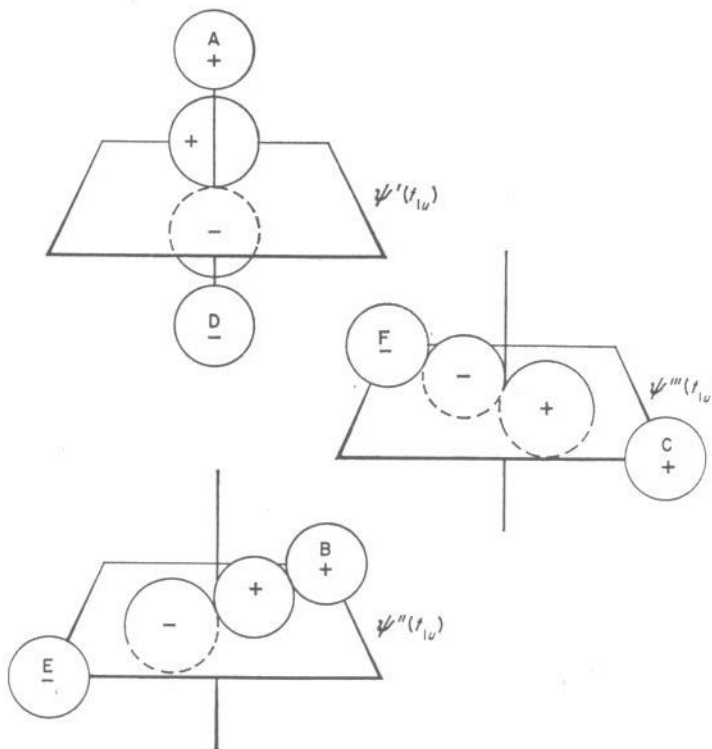
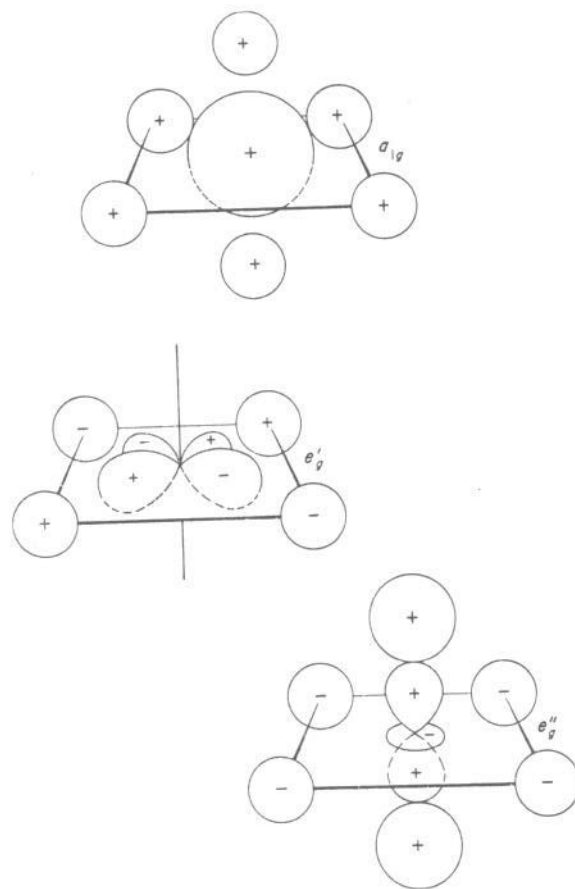


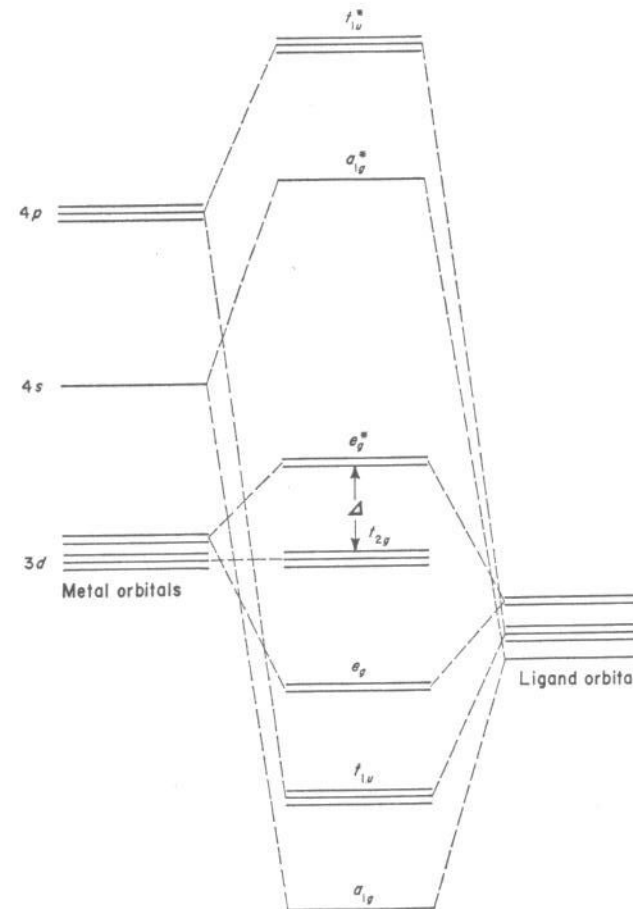
FIGURE 13.11. The t_{1u} ligand orbitals

supported by experiment, which shows that the molecular orbitals which contain unpaired electrons are mainly localized on the metal. The order of the antibonding t_{1u} and a_{1g} is not certain, but as we shall see, this order does not play any part in determining ground state symmetries. We have twelve electrons from the ligands plus any $3d$ electrons from the free ion to allocate to these orbitals. The lowest a_{1g} , t_{1u} and e_g orbitals will be fully occupied in all cases so we can simply consider how the extra electrons are distributed amongst the remaining orbitals which will be t_{2g} and e_g^* in the lowest energy state. This is just what we found with the electrostatic picture (figure 13.2), but we did not recognize the antibonding character of the upper level. Both the electrostatic and the molecular-orbital approaches focus our attention on the separation between the t_{2g} and e_g^* orbitals, which we have called Δ . Everything we said about the states of weak- and strong-field complexes in the section on crystal-field theory will therefore hold also in MO theory.

FIGURE 13.12. The ligand orbitals of a_{1g} and e_g symmetry

We noted that in molecular-orbital theory the t_{2g} orbitals are non-bonding, but if π bonding is important, this is no longer true. Figure 13.14 shows the ligand p orbitals, two on each ligand, which can be involved in π bonding.

These π orbitals can be compounded into ligand group orbitals which, in the O_h group, transform as $T_{1g} + T_{1u} + T_{2g} + T_{2u}$. The precise form of each of these ligand group orbitals could be determined by the same procedure that we used for the σ orbitals. We note that there are no orbitals of T_{1g} and T_{2u} symmetry present in figure 13.13, so these orbitals are non-bonding. Since our real concern is with the t_{2g} and e_g^* orbitals, we may also ignore the t_{1u} ligand π orbitals. We are left with the problem of how the

FIGURE 13.13. Molecular-orbital energy diagram for an octahedral complex.
The asterisks represent antibonding orbitals

ligand group orbitals of symmetry t_{2g} interact with the non-bonding t_{2g} orbitals of figure 13.13. Two cases are likely to occur: (a) the ligand has filled π orbitals which have a lower energy than the $3d$; (b) the ligand has empty π orbitals which have a higher energy than the $3d$. The energy level diagrams in the two cases are shown in figure 13.15. The fluoride ion is an example of case (a), the cyanide ion an example of case (b). Particular notice should be taken of the different effect on Δ shown in figure 13.15. The increase of Δ with π bonding in case (b) probably explains why the cyanide ion heads the spectrochemical series (page 206).

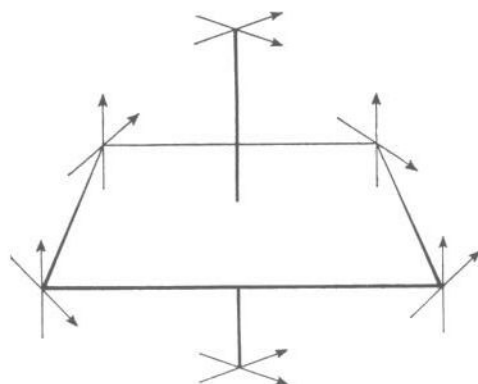


FIGURE 13.14. Ligand $p\pi$ orbitals. The arrows represent their directions, the head of the arrow being the positive end of the orbital

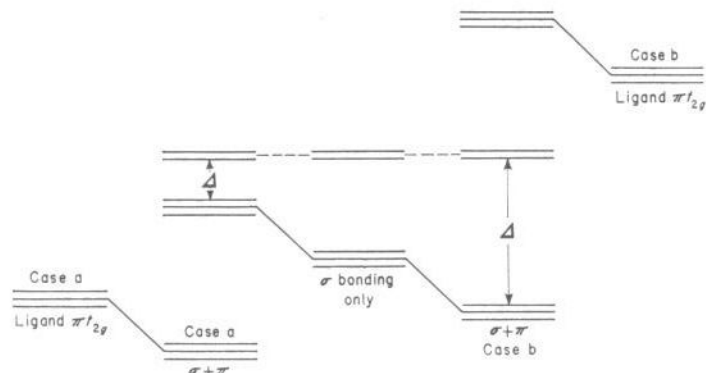


FIGURE 13.15. The effect of ligand orbitals on molecular-orbital energy levels:
(a) ligand has filled π orbitals; (b) ligand has empty π orbitals

13.6 Tetrahedral and planar complexes

We now turn to a discussion of the tetrahedral and square planar stereochemistries which are the only important high-symmetry structures other than the octahedron. Both the octahedron and tetrahedron are related to a cube, as shown in figure 13.16.

Following our discussion of an octahedron, we anticipate that the d orbitals in a tetrahedral field split into sets of two ($d_{x^2-y^2}$ and d_{z^2}) and three (d_{xy} , d_{yz} and d_{zx}). The character table for the group of a regular tetrahedron, T_d , is given in table 13.11. It is instructive to compare this with the character table of the group O_h (table 13.4).

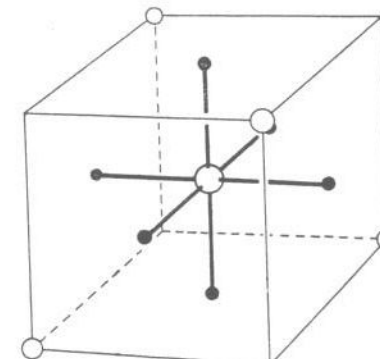


FIGURE 13.16. The relationship between the cube, octahedron and tetrahedron

TABLE 13.11. The T_d character table

T_d	I	$6S_4$	$3C_2$	$6\sigma_d$	$8C_3$
A_1	1	1	1	1	1
A_2	1	-1	1	-1	1
E	2	0	2	0	-1
T_1	3	1	-1	-1	0
T_2	3	-1	-1	1	0

The five d orbitals transform as $E + T_2$, the three p orbitals as T_2 (NOT T_1), and an s orbital as A_1 . Since there is no inversion operation for the tetrahedron, $p-d$ mixing can occur. This will be fairly small and for the moment we ignore it. In figure 13.17 are shown representative d orbitals of E and T_2 species. The lobes of $d_{x^2-y^2}$ are half a cube face

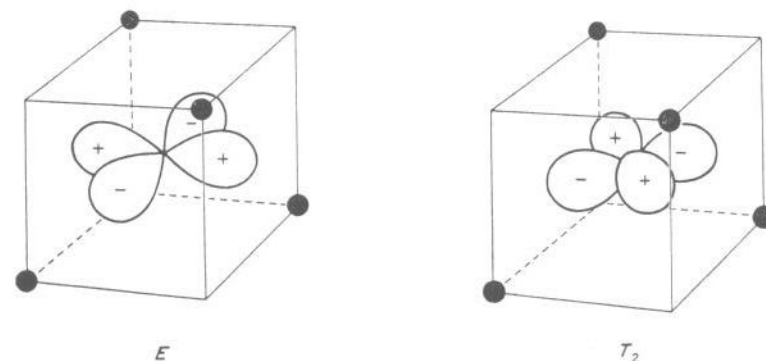


FIGURE 13.17. The representation of orbitals of E and T_2 species in a tetrahedral field

diagonal away from two ligands, those of d_{xy} are half a cube edge away from one. It seems probable that electron-ligand electrostatic repulsion is minimized if the electron occupies the e orbital $d_{x^2-y^2}$, although the splitting must be smaller than in the octahedral case. This is confirmed by calculation, the splitting being $\frac{4}{9}$ of that for the corresponding octahedron. It is most important to note that the t_{2g} orbitals have the lower energy in an octahedron, but the t_2 orbitals have the higher energy in a tetrahedron, i.e.

$$\Delta_{\text{tet}} = -\frac{4}{9}\Delta_{\text{oct}}$$

In figure 13.18 the relationship between the octahedral and tetrahedral splittings is shown for the d^1 configuration. A similar pattern holds for the d^6 configuration; for the d^4 and d^9 configurations the tetrahedral and octahedral patterns are interchanged. A diagram such as figure 13.18 is frequently called an Orgel diagram.

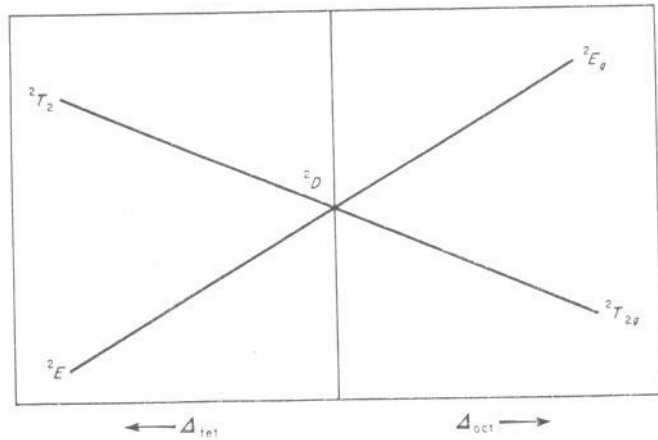


FIGURE 13.18. Orgel diagram for the d^1 configuration

Because Δ_{tet} is only about half of Δ_{oct} for a given ion and ligand, all tetrahedral complexes are high spin (weak field). Crystal-field theory for a tetrahedral complex is exactly the same as for an octahedral complex, but the change in sign of Δ causes all splittings to be inverted. For example, components of the 3F term of the d^2 configuration of an octahedral complex are $^3T_{1g}$ (ground state), $^3T_{2g}$ (first excited state) and $^3A_{1g}$ (second excited state), but for a tetrahedral complex they are 3A_1 (ground), 3T_2 (first excited state) and 3T_1 (second excited state). This means that second-order interaction is larger for tetrahedral than for octahedral d^2 complexes, since the $^3T_1(^3F)$ and $^3T_1(^3P)$ levels are closer together in the former case.

The calculation of the effects of second-order interaction follows (13.17), the sign of terms involving Δ being changed to give energy levels in the strong-field limit at $4X/5 - \Delta/5$ and $X/5 + 4\Delta/5$. An Orgel diagram for the d^2 and related configurations is given in figure 13.19.

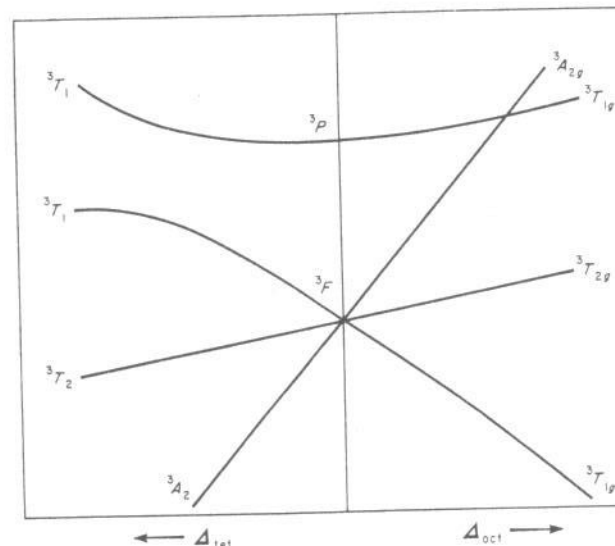


FIGURE 13.19. Orgel diagram for the d^2 configuration

As for an octahedral complex, the 6S term of the d^5 configuration does not split in a tetrahedral ligand field.

Molecular-orbital theory is of considerable importance in the discussion of tetrahedral complexes, since in many of these the metal is in a high valence state (MnO_4^- , MnO_4^{2-} , CrO_4^{2-} , etc.) and considerable delocalization of ligand electrons onto the cation is anticipated. The technique described for the determination of octahedral ligand group orbitals can be used to obtain tetrahedral ligand group orbitals, but the inclusion of the π group orbitals makes the picture rather complex. The ligand σ group orbitals are a_1 and t_2 , and the ligand π group orbitals are $e + t_1 + t_2$. Possible filled molecular orbitals are a_1 , formed from ligand σ and metal s , two t_2 orbitals, from ligand σ and π and metal p and d , an e orbital from ligand π and metal d and the non-bonding t_1 , which is entirely ligand π . Crystal-field theory suggests that the metal d orbitals of t_2 symmetry make a major contribution to the lowest antibonding t_2 molecular orbital (remembering that MO theory identified the e_g orbitals in an octahedral complex as antibonding). It also seems probable that the e molecular

orbital is weakly antibonding. An energy level scheme which satisfies these conditions and which is generally accepted is shown in figure 13.20.

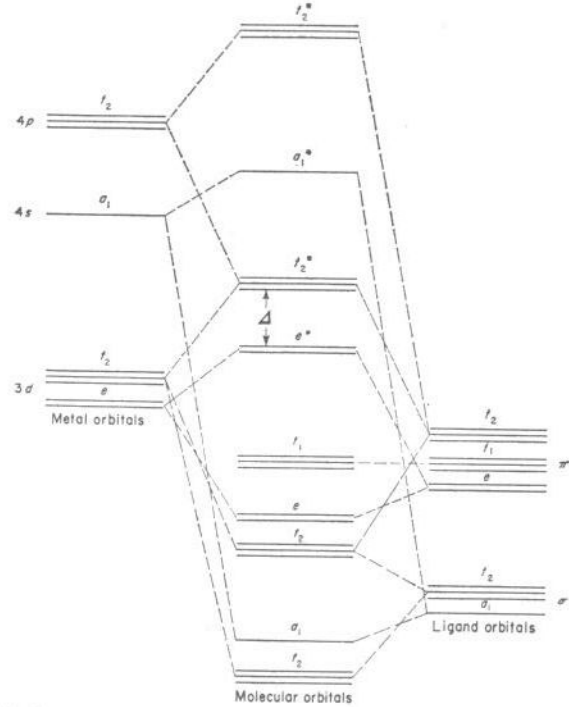


FIGURE 13.20. Molecular-orbital diagram for a tetrahedral complex including π bonding

Square planar complexes are best regarded as the limiting case of tetragonally distorted[†] octahedral complexes. If we take this distortion to be along the z axis then d_{xy} will no longer be degenerate with d_{yz} and d_{zx} although these remain degenerate with each other. The degeneracy between $d_{x^2-y^2}$ and d_{z^2} will also be relieved. Figure 13.21 shows the new splittings for a tetragonal extension and the correlation with the orbitals of a square planar complex.

There is no symmetry reason why δ' and δ'' should be equal. We therefore need two new parameters to discuss the splitting of d orbitals caused by a tetragonal ligand field. From a consideration of the interaction integrals of the tetragonal field it can be shown that $\delta' \approx \delta''$.

[†]i.e. Distorted along a four-fold axis.

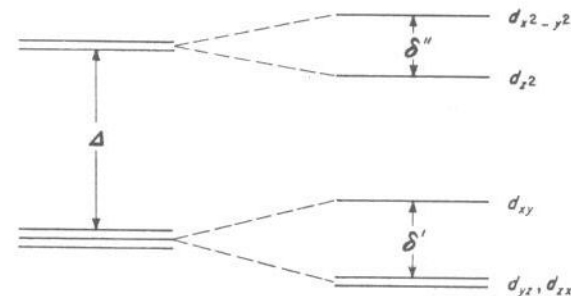


FIGURE 13.21. d orbital splitting for a tetragonal extension of an octahedron

The rule of 'average environment' is a useful aid in the interpretation of the spectra of complexes of lower than cubic symmetry. It is found that the value of Δ for MA_3B_3 is roughly the mean of the Δ 's of MA_6 and MB_6 ; Δ for MA_2B_4 roughly $\frac{1}{3}\Delta(MA_6) + \frac{2}{3}\Delta(MB_6)$, and so on.

13.7 The Jahn-Teller effect

There is a general theorem due to Jahn and Teller which states that if a non-linear molecule is in an orbitally-degenerate state the system will distort so as to relieve that degeneracy. This is illustrated by the following example. Divalent copper is d^9 , and in an octahedral complex the electron configuration would be $t_{2g}^6e_g^3$, which gives rise to a 2E_g state. In this state the hole in the e_g orbitals is as likely to be in the d_z^2 orbital as in the $d_{x^2-y^2}$. The Jahn-Teller theorem requires that the octahedron be distorted so that the degeneracy is removed. If this is done by a tetragonal extension along the z axis then the hole will be localized in $d_{x^2-y^2}$. If there is a tetragonal compression along the z axis the hole will be in d_{z^2} . The Jahn-Teller theorem does not tell us which of these will occur or if some other distortion will occur. Detailed calculations suggest that the tetragonal extension is the most likely, and this is supported by x-ray evidence that axial bonds in octahedral copper complexes are almost always longer than equatorial.

From group theory one can find out how the states appropriate to an octahedral group split up when the symmetry is lowered. This is illustrated for some important cases in table 13.12. What is not obvious at this point is why such splittings will lead to a more stable ground state.

Suppose we start with a regular octahedral complex in its equilibrium configuration. Any distortion of this configuration can be expressed in terms of symmetry distortions R which transform like I.R.'s of the group,

TABLE 13.12. Correlation between the I.R.'s of the octahedral, tetrahedral and lower symmetry groups

O_h	T_d	D_{4h}	D_{3d}	D_{2d}
A_{1g}	A_1	A_{1g}	A_{1g}	A_1
A_{2g}	A_2	B_{1g}	A_{2g}	B_1
E_g	E	$A_{1g} + B_{1g}$	E_g	$A_1 + B_1$
T_{1g}	T_1	$A_{2g} + E_g$	$A_{2g} + E_g$	$A_2 + E$
T_{2g}	T_2	$B_{2g} + E_g$	$A_{1g} + E_g$	$B_2 + E$
A_{1u}	A_2	A_{1u}	A_{1u}	B_1
A_{2u}	A_1	B_{1u}	A_{2u}	A_1
E_u	E	$A_{1u} + B_{1u}$	E_u	$A_1 + B_1$
T_{1u}	T_2	$A_{2u} + E_u$	$A_{2u} + E_u$	$B_2 + E$
T_{2u}	T_1	$B_{2u} + E_u$	$A_{1u} + E_u$	$A_2 + E$

these symmetry distortions being linear combinations of bond stretching and bending coordinates. For example, the A_{1g} symmetry coordinate is

$$R(A_{1g}) = \frac{1}{\sqrt{6}} \sum_{i=1}^6 X_i,$$

where X_i is the change in length of the i^{th} bond. If the Hamiltonian for the undistorted molecule is \mathcal{H} , then, using a Taylor expansion, that of the distorted molecule is

$$\mathcal{H}' = \mathcal{H} + \sum_k \left(\frac{\partial \mathcal{H}}{\partial R_k} \right) R_k + \text{terms in } R^2.$$

One now writes the wave functions of the distorted molecule as a linear combination of those for the undistorted molecule, and solves the secular determinant $|\mathcal{H}'_{rs} - ES_{rs}| = 0$. It is then found that there is at least one symmetry coordinate R_k which appears in the energy of the lowest state in linear form (or something that is equivalent to linear like $[R_{k_1}^2 + R_{k_2}^2]^{\frac{1}{2}}$, where R_{k_1} and R_{k_2} are components which together transform like a degenerate I.R. of the group). This means that superimposed on the normal quadratic form of the potential energy curve there will be a linear term in the displacement, so that the energy minimum no longer corresponds to the regular octahedral configuration.

It is only in the case of unequal occupation of the e_g orbitals that the Jahn-Teller effect is of recognized importance in the chemistry of transition metal complexes. Although unequal occupation of the t_{2g} orbitals must lead to a distortion, the non-bonding character of these orbitals suggests that any distortion of the complex will be small. In practice there are usually other mechanisms for relieving the degeneracy of these orbitals (spin-orbit coupling or crystal forces, for example).

If a Jahn-Teller distortion energy is of the same order of magnitude as a zero-point vibration energy, then there is no permanent distortion of the molecule. This situation is associated with a breakdown of the Born-Oppenheimer approximation and is referred to as the dynamic Jahn-Teller effect.

13.8 The electronic spectra of transition metal complexes

The visible and ultraviolet spectra of transition metal complexes show three types of band

- (a) sharp, weak;
- (b) broad, weak;
- (c) broad, strong.

The first two of these are accounted for by crystal-field theory, the third requires ligand-field theory.

The weak bands are all associated with forbidden electronic transitions involving the excitation of an electron from one d orbital to another—a $g \rightarrow g$ transition (see page 120). The relative positions of these weak bands are readily correlated with energy level diagrams such as are shown in figures 13.6–13.9.

The strong broad bands which generally appear at the short wavelength end of the spectrum are due to transitions of an electron from one of the bonding molecular orbitals (largely located on the ligands) to either an e_g or t_{2g} orbital (largely located on the metal). These transitions are accompanied by a charge migration from the ligand to the metal and are called charge-transfer transitions (see chapter 18). They have not been greatly studied, although for some complexes a correlation has been found between peak position and the nature of the ligand.

The spectra of weak-field complexes are the easiest to interpret quantitatively. For the intermediate case, which occurs frequently in practice, second-order interactions are important and large secular determinants may have to be solved—for example, the $10 \times 10^2 T_2(d^5)$ determinant already mentioned[†].

We shall discuss the spectra of two ions, $[\text{Ti}(\text{H}_2\text{O})_6]^{3+}$ and $[\text{V}(\text{H}_2\text{O})_6]^{3+}$ (d^1 and d^2 configurations respectively). The spectrum of $[\text{Ti}(\text{H}_2\text{O})_6]^{3+}$ is shown in figure 13.22. It contains one weak peak at $20,300 \text{ cm}^{-1}$, ascribed to the ${}^2T_{2g} \rightarrow {}^2E_g$ transition, and this is the value of Δ in wavenumbers. In most octahedral complexes of Ti^{3+} this peak carries a shoulder, sometimes

[†] The interaction matrices are given by TANABE and SUGANO, *J. Phys. Soc. Japan*, **9**, 753 (1954) and by McClure, *Solid State Phys.* **9**, 399 (1959), and one has only to substitute the numbers appropriate to the ion under consideration. The solution of these large secular determinants is a job for a computer.

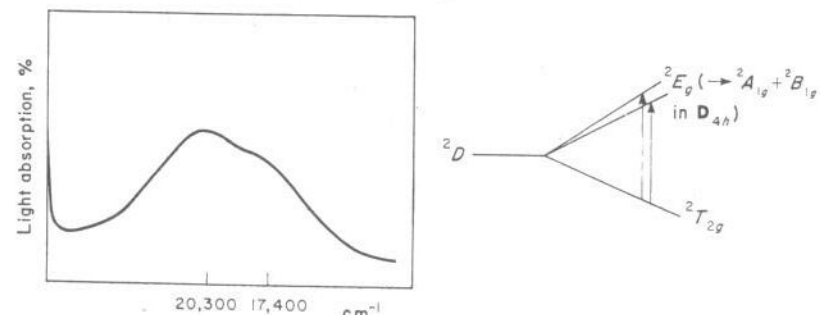


FIGURE 13.22. The absorption spectrum of $[\text{Ti}(\text{H}_2\text{O})_6]^{3+}$ and its interpretation

almost resolvable as a separate peak. This is probably because the excited level shows a Jahn-Teller distortion since there is only one electron in the e_g^* orbitals. $[\text{V}(\text{H}_2\text{O})_6]^{3+}$ has the spectrum shown in figure 13.23. It consists of two weak peaks at 17,100 and 25,200 cm^{-1} assigned to $^3T_{1g} \rightarrow ^3T_{2g}$ and $^3T_{1g} \rightarrow ^3T_{1g}$ transitions.

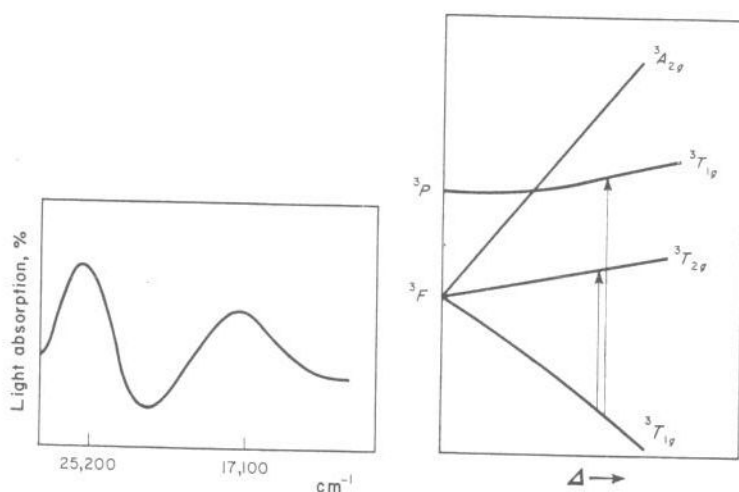


FIGURE 13.23. The absorption spectrum of $[\text{V}(\text{H}_2\text{O})_6]^{3+}$ and its interpretation

Using the formulae derived earlier (page 219 and table 13.6), we have

$$E(^3T_{1g} \rightarrow ^3T_{1g}) = (X^2 + (\frac{6}{5})\Delta X + \Delta^2)^{\frac{1}{2}} = 25,200 \text{ cm}^{-1},$$

$$E(^3T_{1g} \rightarrow ^3T_{2g}) = -\frac{1}{2}X + (\frac{1}{2}\Delta) + \frac{1}{2}(X^2 + (\frac{6}{5})\Delta X + \Delta^2)^{\frac{1}{2}} = 17,100 \text{ cm}^{-1},$$

which have solutions $\Delta = 16,700 \text{ cm}^{-1}$ and $X = 11,800 \text{ cm}^{-1}$. This value of X is to be compared with that of the $^3F-^3P$ separation of the free ion which is $13,200 \text{ cm}^{-1}$. The agreement between these two figures is a measure of the validity of the crystal-field approximations. The predicted $^3T_{1g} \rightarrow ^3A_g$ transition is at $34,100 \text{ cm}^{-1}$ where it is obscured by a strong charge-transfer band.

It is seen from figure 13.8 that for a d^3 configuration three of the excited states have about the same dependence on Δ as the ground state whereas others have a very different dependence on Δ . Since Δ is modulated by thermal vibrations of the ligands (a compressed complex will have a larger, and a stretched complex a smaller Δ), we expect that the transitions such as $^4A_{2g} \rightarrow ^2E_{2g}$, whose energies are almost independent of Δ , will give sharper bands than, say, $^4A_{2g} \rightarrow ^4T_{2g}$, whose energy is very sensitive to Δ . This phenomenon is well illustrated by the crystal spectrum of ruby (Cr_2O_3 , Al_2O_3), which is given in figure 13.24. All sharp bands are spin forbidden, because the ground and excited states have the same occupation of e_g and t_{2g} orbitals (this is why their energies have the same dependence on Δ) and only differ in their spin multiplicity. However, the converse is not true; not all spin-forbidden transitions give rise to sharp bands.

It is believed that the intensity of weak absorption bands is largely due to $d-p$ mixing. If $d-p$ mixing occurs $d \rightarrow d$ transitions take on some $d \rightarrow p$ and $p \rightarrow d$ character, both of which are allowed transitions for the free ion

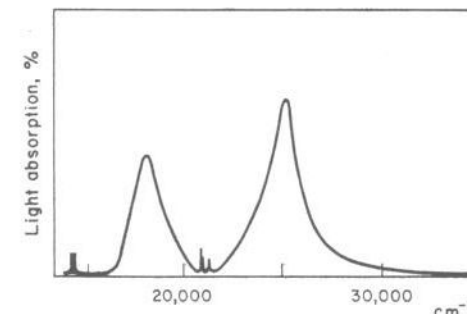


FIGURE 13.24. The absorption spectrum of ruby

and the complex. In tetrahedral complexes, for example, the p and three of the d orbitals transform as T_2 so that mixing is allowed. Tetrahedral complexes tend to have much more intense absorption than octahedral—the manganate ion is a good example of a tetrahedral complex with a strong absorption. Another useful comparison is $[\text{CoCl}_4]^{2-}$ (deep blue) and $[\text{Co}(\text{H}_2\text{O})_6]^{2+}$ (pale pink). This still does not explain the spectra of

strictly octahedral complexes, for which d - p mixing is not possible. However, our model is defective because it takes no account of the vibrations of the molecule. Some of these vibrations reduce the symmetry and in this reduced symmetry d - p mixing is allowed. The intensity of an absorption band should really be calculated by averaging over all configurations taken up by the molecule during the vibrations.

Transitions between states of different spin multiplicity are forbidden in the absence of spin-orbit coupling (page 119). In the presence of spin-orbit coupling S ceases to be a good quantum number, and transitions between states of different spin multiplicity give rise to weak absorption bands.

There are other physical properties which can shed much light on the nature of metal complexes. Firstly, magnetic measurements, both of bulk susceptibility and of electron-spin resonance, can give direct evidence on the symmetry of the ground state. Secondly, a study of the absorption of polarized light by a single crystal, and, for optically active complexes, a study of the circular dichroism or optical rotary dispersion spectra, will give added information about excited states. Although these techniques are extremely important, we feel they are rather outside the scope of this book.

13.9 Conclusions

It has been the object of this chapter to describe the techniques of ligand-field theory rather than to give a critical appraisal of it. Crystal-field theory has obvious deficiencies all based on the fact that it allows for no delocalization of the d electrons. On the other hand, a non-empirical MO theory is completely out of the question with the techniques at present available, and the qualitative results obtained from MO theory parallel those obtained from crystal-field theory.

Because of the inherent simplicity of crystal-field theory it is useful to ask how it should be changed to allow for electron delocalization. The answer is that three quantities need to be modified. The first are the electron repulsion integrals. These need to be reduced because covalency spreads out the electrons and therefore reduces their repulsion. In practice a reduction of up to 30% of the free-ion value may be required, as we saw in the calculation in the V^{3+} spectrum. Ligands can be arranged in a series, the Nephelauxetic (cloud-expanding) series, such that the electron repulsion parameters decrease from left to right, as covalency increases:



Secondly, the spin-orbit coupling constant is reduced below the free-ion value. This is to be expected if an electron spends some of its time in ligand orbitals where coupling between its spin and the (metal) orbital angular momentum will be small. This reduction may also be of the order of 30%. Thirdly, in a detailed calculation of magnetic susceptibility the orbital contribution to the magnetic moment (9.10) must be reduced, for the same reason that the spin-orbit coupling is reduced. These reductions increase the empirical nature of crystal-field calculations, but do not detract from the great success which the theory has had in correlating a vast amount of spectral, magnetic, thermodynamic and kinetic data.

Bibliography

- ORGEL, *An Introduction to Transition Metal Chemistry*, Methuen and Wiley, 1960.
- BALLHAUSSEN, *Introduction to Ligand Field Theory*, McGraw-Hill, 1962.
- GRIFFITH, *The Theory of Transition Metal Ions*, C.U.P., 1961.
- MOFFITT and BALLHAUSSEN, *Ann. Rev. Phys. Chem.*, 7, 107 (1956).
- LOW, *Paramagnetic Resonance in Solids*, Academic Press, 1960.

Problems 13

- 13.1 The complex ion $[FeF_6]^{3-}$ is colourless. How many unpaired electrons would you expect it to have?
- 13.2 Show that the F states arising from a d^n configuration split up in an octahedral field to give T_{1g} , T_{2g} and A_{2g} components.
- 13.3 Write down the eigenfunctions of the ground state for d^8 and d^9 octahedral complexes in terms of atomic state wave functions (cf. table 13.6) and in terms of real d orbitals.
- 13.4 Assign the peaks in the visible spectra of $[Mn(H_2O)_6]^{2+}$ given below.

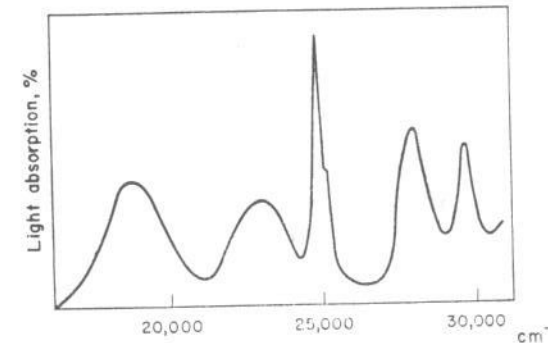


FIGURE 13.25. The absorption spectrum of $[Mn(H_2O)_6]^{2+}$